Steel and Composite Structures, *Vol. 20, No. 1 (2016) 167-184*
DOI: http://dx.doi.org/10.12989/scs.2016.20.1.167

Numerical evaluation of deformation capacity of laced steel-concrete composite beams under monotonic loading

A. Thirumalaiselvi [*], N. Anandavalli [a], J. Rajasankar [b] and Nagesh R. Iyer [c]

Academy of Scientific and Innovative Research;
CSIR-Structural Engineering Research Centre, *CSIR Campus*, *Taramani*, *Chennai 600 113*, *India*

(*Received November 24, 2014, Revised August 07, 2015, Accepted September 09, 2015*)

Abstract. This paper presents the details of Finite Element (FE) analysis carried out to determine the limiting deformation capacity and failure mode of Laced Steel-Concrete Composite[†] (LSCC) beam, which was proposed and experimentally studied by the authors earlier (Anandavalli *et al*. 2012). The present study attains significance due to the fact that LSCC beam is found to possess very high deformation capacity at which range, the conventional laboratory experiments are not capable to perform. FE model combining solid, shell and link elements is adopted for modeling the beam geometry and compatible nonlinear material models are employed in the analysis. Besides these, an interface model is also included to appropriately account for the interaction between concrete and steel elements. As the study aims to quantify the limiting deformation capacity and failure mode of the beam, a suitable damage model is made use of in the analysis. The FE model and results of nonlinear static analysis are validated by comparing with the load-deformation response available from experiment. After validation, the analysis is continued to establish the limiting deformation capacity of the beam, which is assumed to synchronise with tensile strain in bottom cover plate reaching the corresponding ultimate value. The results so found indicate about 20° support rotation for LSCC beam with 45° lacing. Results of parametric study indicate that the limiting capacity of the LSCC beam is more influenced by the lacing angle and thickness of the cover plate.

Keywords: steel-concrete composite construction; shear connector; finite element analysis; concrete damage plasticity model; static response

1. Introduction

Behaviour of Steel-Concrete Composite (SCC) structural components is strongly governed by interaction and force transfer between steel and concrete elements (Clubley *et al*. 2003a). Transfer of forces between steel and concrete elements is realised by means of shear connectors to achieve the composite action. Shear connectors, are in general, welded to the steel cover plates (Machacek and Studnicka 2002) and their effectiveness to transfer force depends mainly upon the strength of welding of shear connectors to the cover plates (Luo *et al*. 2012). Number and spacing of shear

*Corresponding author, Senior Project Fellow, E-mail: selvi@serc.res.in; selvi1056@gmail.com
[a] Principal Scientist
[b] Chief Scientist
[c] Distinguished Emeritus Professor
[†] Indian Patent filed-1886DEL2011dated 05.07.2011

http://www.techno-press.org/?journal=scs&subpage=8 ISSN: 1229-9367 (Print), 1598-6233 (Online)

connectors are a function of the magnitude of force to be transferred. Capacity of SCC components is decided primarily by weld strength (Clubley *et al*. 2003b). SCC structures are adopted in situations that require high strength, ductility as well as energy absorbing capacity to resist applied loads (Sohel *et al*. 2003).

A promising research trend in SCC construction is to develop new form of shear connectors. Headed shear stud connector is used in Double Skin Composite (DSC) construction (Tomlinson *et al*. 1989). Difficulty with on-site control, especially controlling the depth of the composite core in the unfilled stage is typically encountered with this type of connector. Overcoming this difficulty, a through-through type shear connector was proposed by Bowerman *et al*. (2002). However, this type also suffers from the drawback that the thickness of the core must be sufficient enough to place the connector. In addition to these two types of SCC construction, two more alternative SCC constructions were proposed recently such as SCC system with J-hook connectors (Liew and Sohel 2009, Liew *et al*. 2009) and SCC beam with bi-directional corrugated-strip-core system (Leekitwattana 2011). In all of the above SCC systems, shear connectors are welded to the steel cover plates.

Laced Steel-Concrete Composite (LSCC) system is a novel form of SCC system developed recently by the authors (Anandavalli *et al*. 2012). LSCC system consists of perforated steel cover plates, which are connected using reinforcing members and cross rods and in-filled with concrete as shown in Fig. 1. Reinforcing member consists of continuously bent rods known as lacing, which transfer the force between steel cover plate and in-filled concrete. LSCC is devoid of welding due to particular arrangement of lacings being inserted through the perforations in the cover plate at appropriate places and made to stay intact by using cross rods. Forces in top and bottom cover plates together act as a couple and resist the moment generated due to external forces.

As LSCC system consists of simple structural members arranged in a novel manner, it will be of research interest to know the overall system behaviour including the failure mechanism. For this purpose, two LSCC beam specimens are subjected to two point monotonic loading under a typical loading arrangement (Anandavalli *et al*. 2012). During experiment, two beams had exhibited large deformation. In particular, the post-peak response is found to exhibit only minimum drop in the load value over a large range of deformation. The experiment had to be discontinued in order to avoid the risk of support rod slipping at such large deformation. The beam specimen is found to deform to an extent of realising about 16° rotation at the supports. This is very high value compared to a rotation of only about 3.5° for reinforced concrete (RC) beam. As the experiment was discontinued abruptly due to safety considerations, the maximum capacity and the failure mechanism could not be ascertained. The motivation for the present investigation is derived from the need to understand the limiting capacity of LSCC beams and also associated failure

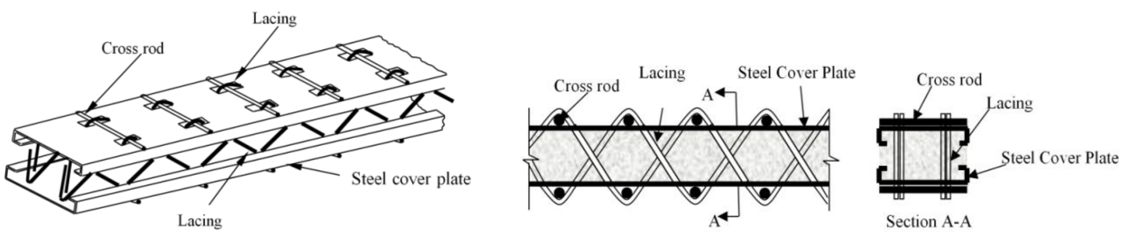

(a) (b)

Fig. 1 (a) Isometric view of LSCC configuration; (b) Cross-section of LSCC system mechanism under monotonic loading. Further, the numerical study gains significance as conventional laboratory experiments cannot be conducted at such large deformation range.

FE model, which is capable of predicting complete nonlinear response of LSCC system is developed using the FE analysis software ABAQUS and described in this paper. Solid-shell-link approach is adopted to represent concrete core, steel cover plate, lacings and cross rods. Concrete damage plasticity model is used to represent nonlinear behaviour of concrete including strain softening. Bi-linear material model is adopted to represent steel behaviour. The interface between cover plate and in-filled concrete is defined by surface to surface interaction technique. Friction formulation in tangential direction and hard contact in normal direction is provided between the interacting surfaces. The results obtained by using FE model are found to match well with the experimental values even beyond peak load level. Thus, the proposed FE model provides a framework to obtain the complete load-deformation behaviour of LSCC beams. Mainly, the aim of understanding the limiting capacity and failure mechanism of LSCC beam is achieved through the FE model. Taking lacing angle, cover plate thickness and concrete grade into account, parametric study is conducted and the element which influences the response of LSCC beams under monotonic loading is determined.

2. Geometry and load details: LSCC beam

Monotonic load testing under two point loading has been conducted earlier on two LSCC beam specimens, one with 45° lacing angle and another with 60° lacing angle, under displacement control mode by Anandavalli *et al*. (2012). The specimens have been tested with simply supported boundary conditions. A LSCC beam with similar dimensions is modelled by using FE analysis software ABAQUS. The geometrical and material property values of the LSCC beam are given in Tables 1 and 2 respectively. Schematic diagram of two point loading set-up is shown in Fig. 2.

Table 1 Geometry details of LSCC beam (Anandavalli 2012)

Details	Description	Value
LSCC beam	Length, mm	2400
	Span (between supports), mm	1800 (LSCC-45 beam) 1950 (LSCC-60 beam)
	Shear span, mm	665 (LSCC-45 beam) 610 (LSCC-60 beam)
Concrete core	Width, mm	300
	Depth, mm	150
Steel cover plate	Width, mm	300
	Thickness, mm	4
Lacings	Diameter, mm	8
	Transverse spacing, mm	200
	Angle of lacing, degrees	45,60
Crossrod	Diameter, mm	10
	Total number of crossrods (on top and bottom)	32 (LSCC-45 beam) 62 (LSCC-60 beam)

Table 2 Material property values of LSCC beam (Anandavalli 2012)

Details	Description	Value
Concrete core (Concrete)	Elastic modulus, MPa	35443.7
	Poisson's ratio	0.19
	Compressive strength, MPa	56
Steel cover plate (Cold formed steel)	Elastic modulus, MPa	200000
	Poisson's ratio	0.25
	Average yield stress, MPa	190
	Ultimate stress, MPa	300
Lacings and cross rod (High strength bars)	Average yield stress, MPa	400
	Ultimate stress, MPa	540

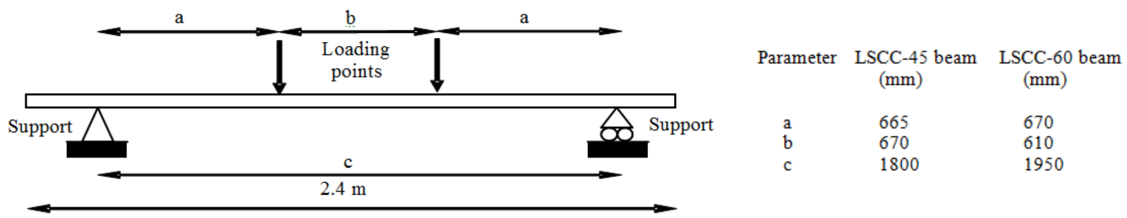

Fig. 2 Loading arrangement on LSCC beam

3. Finite element analysis

The accuracy of numerical model depends mainly on the capability of simulating actual material behaviour and interface contact between steel and concrete. Conventional way of modeling the SCC system is to employ solid elements to discretise all the components, namely, steel, concrete and shear connector. Finite element analysis of bi-steel has been carried out by Clubley *et al*. (2003a) using 3D elements to represent all components, smeared contact elements to simulate contact between the side plates, concrete face and discrete contact elements to simulate contact on surface of shear connectors. Modeling using a combination of smeared and discrete contact elements at interface between steel and concrete surfaces had been proved to predict its physical behaviour accurately (Clubley *et al*. 2003a). However, modeling using 3D elements results in complicated problem. To overcome problems arising due to complex model and high computational requirement, different modeling techniques are being adopted in recent years. Compromising stress variation in the third dimension normal to the plane of the beam, SCC beam modeling has been made in 2D space and load-deflection values up to maximum load was found to match with test results (Foundoukas and Chapman 2008). Without any such compromise, a computationally efficient modeling technique using solid-shell-link approach was proposed by Anandavalli *et al*. (2011) and it was proved to be less demanding on modeling requirements besides capable of producing accurate results. By this approach, solid, shell and link elements are used to represent the concrete core, steel plates and shear connectors respectively. Therefore, in the present study, solid-shell-link approach has been adopted to model LSCC system.

3.1 FE model of LSCC beam

As explained earlier solid and shell elements are used to model concrete core and steel cover plates respectively. Eight-node brick elements with reduced integration (C3D8R) are used to model concrete core, while four-node shell elements with reduced integration (S4R) are used to model steel cover plates and two-node linear beam elements (B31) are used to represent lacings and cross rods.

Two point loading is adopted with loads applied at the nodes at 665 mm and 1035 mm distance from left support on the top plate. The load applied on the top surface of steel cover plate is distributed over full width of the beam. Likewise, simply supported boundary conditions are simulated as shown in Fig. 2 in such a way that reaction forces at the supports are distributed throughout the width of the beam.

3.2 Constitutive material models

The full range nonlinear analysis of LSCC beams under monotonic loading requires detailed knowledge of the stress-strain relationship of concrete and steel. Stress-strain curve of concrete in compression including strain softening has been modelled by using empirical relationship developed by Attard and Setunge (1996). This stress-strain relationship for confined concrete was empirically developed based on standard tri-axial tests conducted on five mixes with three types of aggregate. This model was shown to be applicable to a broad range of in-situ concrete strength from 20 to 130 MPa (Au and Bai 2007). The model is expressed by following Eq. (1)

$$\frac{\sigma_c}{f_{co}} = \frac{A(\varepsilon_c/\varepsilon_{co}) + B(\varepsilon_c/\varepsilon_{co})^2}{1+(A-2)(\varepsilon_c/\varepsilon_{co}) + (B+1)(\varepsilon_c/\varepsilon_{co})^2} \tag{1}$$

where σ_c is the stress of concrete, ε_c is the strain of concrete, f_{co} is the peak compressive stress and ε_{co} is the corresponding strain, A and B are coefficients depending on the concrete grade

Two sets of the coefficients A and B are required, with one for the ascending branch and another for the descending branch of the curve. For the ascending branch, where $\sigma_c \le f_{co}$ coefficients A and B are given by

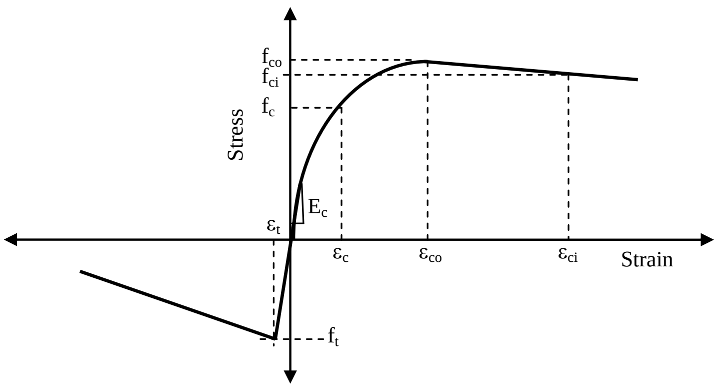

Fig. 3 Stress-strain behaviour of concrete

$$A = \frac{E_c \varepsilon_{co}}{f_{co}}; \qquad B = \frac{(A-1)^2}{0.55} - 1 \tag{2}$$

Two sets of the coefficients *A* and *B* are required, with one for the ascending branch and another for the descending branch of the curve. For the ascending branch, where $\sigma_c \leq f_{co}$ coefficients *A* and *B* are given by

$$A = \frac{f_{ci}(\varepsilon_{ci} - \varepsilon_{co})^2}{\varepsilon_{co}\varepsilon_{ci}(f_{co} - f_{ci})}; \qquad B = 0 \tag{3}$$

where E_c is the initial Young's modulus, f_{ci} and ε_{ci} are the compressive stress and corresponding strain at the inflection point on the descending branch of the curve.
The parameters E_c, f_{co}, f_{ci} and ε_{ci} are theoretically related to the value f_{co} by

$$\begin{aligned} E_c &= 43700(f_{co})^{0.52} \\ \varepsilon_{co} &= 4.11(f_{co})^{0.75} / E_c \\ f_{ci} / f_{co} &= 1.41 - 0.17\ln(f_{co}) \\ \varepsilon_{ci} / \varepsilon_{co} &= 2.50 - 0.30\ln(f_{co}) \end{aligned} \tag{4}$$

Stress–strain relationship for concrete in tension assumes that the tensile stress increases linearly with tensile strain upto concrete cracking stress. After cracking of concrete, the tensile stress decreases as the concrete softens. Post-peak stress-strain behaviour in tension is defined by using tension stiffening option. To consider the post-cracking resistance in tension, the model proposed by Guo and Zhang (1987) is adopted, namely

$$\frac{\sigma_c}{f_t} = \frac{-\varepsilon_c / \varepsilon_t}{\gamma(\varepsilon_c / \varepsilon_t - 1)^{1.7} + (\varepsilon_c / \varepsilon_t)} \tag{5}$$

where f_t is the tensile strength, ε_t is the strain at tensile strength, γ is a dimensionless coefficient equals to 0.312 f_t^2.

Nonlinear behaviour of steel is modelled using plasticity model available in the software. The uniaxial tensile stress-strain behaviour of various steels used in the LSCC beam is explained in following sub sections.

(a) Steel cover plate

Steel cover plates are made of cold-formed steel. Details of tensile test of three coupons fabricated from same sheets as cover plates (Anandavalli 2012) are taken, and the corresponding stress-strain curve adopted is shown in Fig. 4. Coupons are found to fail at around 20% strain value.

Nonlinear material model is employed based on the nominal stress-strain behaviour of steel as shown in Fig. 5. The stress and the corresponding plastic strain values computed from the actual strain values are given as input in the finite element analysis software.

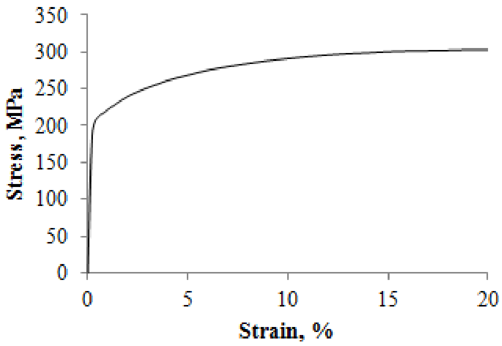

Fig. 4 Stress-strain curve of cold-formed steel

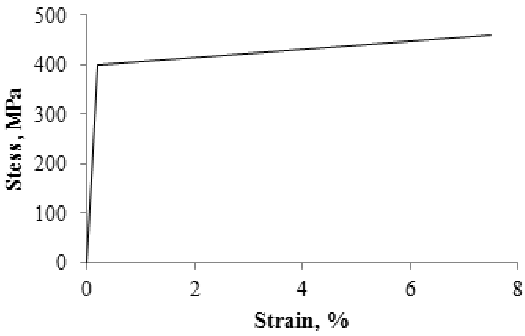

Fig. 5 Stress-strain curve of reinforcing steel

(b) Lacings and cross rods

Lacings and cross rods are made of reinforcing steel. Details of tensile test of reinforcing bars (Anandavalli 2012) are taken and idealized bi-linear stress-strain curve is adopted. Bi-linear stress-strain behaviour as shown in Fig. 5 is given as input to the model. When the strain ε_s increases, the stress σ_s in the steel is given by

$$\sigma_s = E_s \varepsilon_s, \quad \text{for} \quad \varepsilon_s \leq f_y / E_s \quad \text{(at elastic stage)}$$

$$\sigma_s = \sigma_y + \frac{(f_u - f_y)}{(\varepsilon_u - \varepsilon_y)}(\varepsilon_u - \varepsilon_y) \quad \text{(after yielding, till ultimate)} \tag{6}$$

The yield and ultimate stress values are given in Table 2.

3.3 Damage model

ABAQUS software provides the ability of simulating the damage using either of the three damage models for concrete elements: (1) Smeared crack concrete model; (2) Brittle crack concrete model; and (3) Concrete damaged plasticity model. Among these, concrete damaged plasticity (CDP) model is selected in the present study as this technique has the potential to represent complete inelastic behaviour of concrete both in tension and compression including damage characteristics. The advantage of CDP model is due to the fact that it is mainly based on parameters having an explicit physical interpretation. The CDP model is a modification of the Drucker–Prager strength hypothesis. The CDP model has proven to provide proper definition of the failure mechanisms in concrete elements (Jankowiak and Lodygowski 2005).

3.4 Mechanical interaction model

Mechanical interaction between the steel cover plate and concrete surfaces is modelled by surface to surface contact interactions using friction formulation in tangential direction and hard contact in normal direction. Surface to surface contact interaction technique available in the software defines the contact between two surfaces i.e., steel cover plate and concrete core surfaces. Hard contact is provided in normal direction to avoid penetration of steel surface into concrete surface. Hard contact also implies that contact pressure can be transmitted only when the steel and concrete surfaces are in contact and the separation is allowed after contact in the interaction model. Interaction provided between steel and concrete surfaces is schematically shown in Fig. 6. The classical coulomb friction model is adopted to characterize the frictional behaviour between the surfaces. In this model, two surfaces which are in contact can carry shear stresses only upto certain magnitude across their interface before they start sliding relative to each other. Coulomb friction model is defined as

$$\tau_{\lim} = \mu P \tag{7}$$

where $\tau_{\lim}$ is the limiting shear stress, μ is the coefficient of friction and P is the normal contact pressure.

Contact constraints are enforced using penalty method. Penalty method introduces additional stiffness behaviour into the model. The penalty method has been implemented such that no Lagrange multipliers (as used in case of Lagrangian method) are used, which allows for improved solver efficiency. This method is used for tangential behaviour along with the coefficient of friction as 0.4. Node to surface interaction is given between nodes of crossrods and steel plate. Finite sliding along with penalty contact method is used for the interaction between crossrod and steel plate. For interaction between concrete core and steel cover plate, the concrete surface is modelled as slave and surface of steel plate is modelled as master.

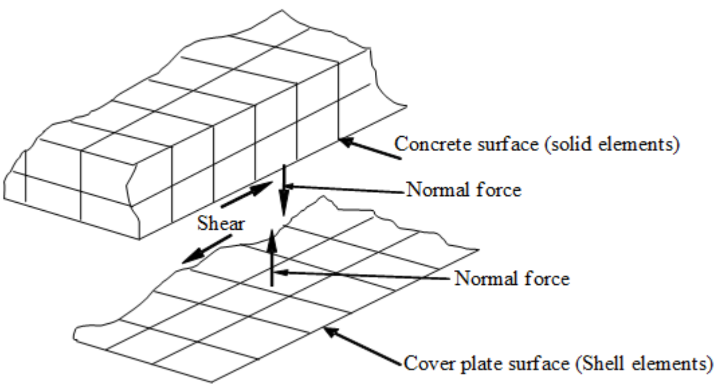

Fig. 6 Interaction between steel and concrete surfaces

(a) Concrete core (b) Steel plates with lacings

Fig. 7 Finite element model of LSCC beam

Common nodes of steel plate and lacings are merged. Lacings are connected with cross rods at intersecting nodes. Connection of weld provides a fully bonded connection between two nodes. Lacings are embedded in concrete. The embedded element technique is used to specify an element or a group of elements that lie embedded in a group of host elements, whose response will be used to constrain the translational degrees of freedom of the embedded nodes. In this study, truss element in solid embedment model is used.

Salient features of the finite element model and the subsequent analysis are:

(1) Structured mesh
(2) Concrete damage plasticity model for nonlinear material behaviour of concrete and plasticity model for steel
(3) Interface contact applied between cover plate and concrete core surfaces
(4) Nonlinear static analysis
(5) Newton-Raphson solution technique

Three different mesh sizes are tried and convergence study is conducted in arriving at the final FE mesh. It is observed that the load-deflection response obtained using finer mesh size gives good agreement with the experimental results. Hence the final mesh having elements of size 25 mm with aspect ratio 1 as shown in Fig. 7 is chosen for the further analysis.

3.5 Finite element analysis results

Nonlinear static analysis is carried out to obtain its static response under four point bending.

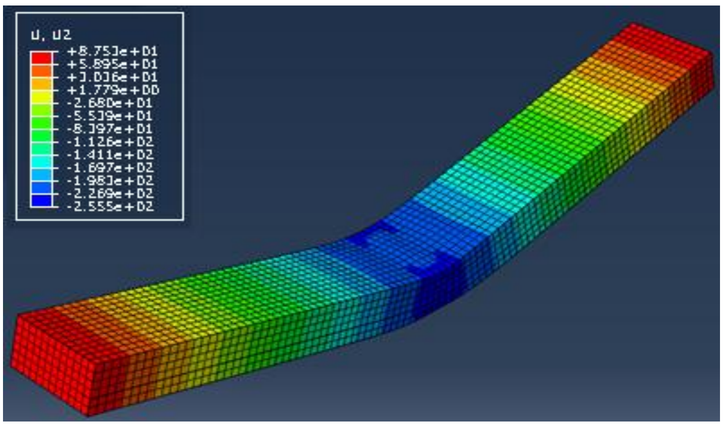

Fig. 8 Deformed contour of LSCC-45 beam

Newton-Raphson solution technique is adopted. Load-deflection behaviour and critical stages of failure are discussed in the following sections. The final deformed shape of LSCC-45 beam at failure stage is shown in Fig. 8. Validation of the finite element model is carried out by using the experimental results available (Anandavalli *et al*. 2012).

3.5.1 Load-Deflection Behaviour of LSCC-45 beam

Load-deflection values of LSCC-45 beam obtained by using FE analysis is shown in Fig. 9. Results obtained using FE model and experimental results are found to match very well.

In the initial elastic region upto about 70 kN, it is observed that both numerical and experimental load-deflection values coincide. With increasing load, FE analysis shows larger deflection as compared to the experimental upto a load value of 133 kN. With further increase in load above 133 kN, the FE model predicts about 20% less deflection than the experimental upto ultimate load. Also, little difference in the post-peak response is observed, when compared with that of experimental value.

The ultimate load obtained by the FE model is found to be 2.62% more than that of the corresponding experimental value (151.3 kN). FE analysis overestimates the load carrying capacity of LSCC beam.

Mainly, it is observed that FE model is able to predict the post-peak response of LSCC beam more appropriately. In general, post-peak response of structural system is of great interest in situations, when it is subjected to suddenly applied loads of very high magnitude. Experiment has been stopped in between due to safety considerations. Experimentally, it is found to have 2% drop in the load for maximum mid-span displacement of about 170 mm. From numerical analysis, the drop in the load for maximum mid-span displacement of about 255 mm is found to be approximately 5%.

Moreover, using FE model, ultimate failure point has been arrived. Tension plate failure is considered as the failure mode. Failure point is ascertained by measuring the strain in individual components. Ultimate failure has not been ascertained in experiments due to reasons explained earlier. It is observed that area under the load-deflection curve (energy absorbed) obtained using FE analysis is 50% more than that obtained by using experiments. Thus actual energy absorption capacity is obtained and this plays an important role in dealing with the nonlinear response of structures subjected to severe loading cases.

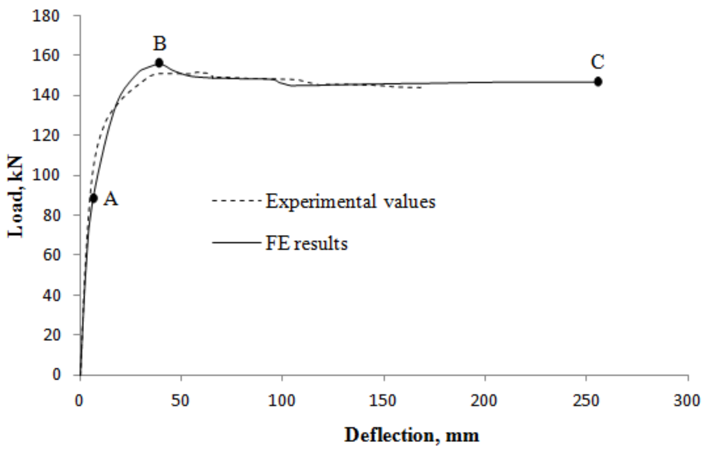

Fig. 9 Load-deflection behaviour of LSCC-45 beam

Support rotation is calculated by using the relation $\theta = \tan^{-1}\left(\frac{\delta}{a}\right)$, where δ = deflection under the loading point and a = distance of support end from loading point. Since the experiment has been stopped in between (before failure is arrived), the deflection recorded at the instant is 177 mm and the corresponding support rotation is determined to be about 13°. Numerically it is found that LSCC beam can take larger deflection than that recorded in experiments since failure point is arrived in numerical analysis and the deflection at failure is found to be around 250 mm, support rotation is approximately calculated to be 20°. From FE analysis, ductility index (the ratio of ultimate deflection to the corresponding yield deflection) of LSCC beam is calculated to be around 32, which is approximately 35% more than that obtained using experiments.

Table 3 Comparison of strain values in cover plates at maximum load of LSCC-45 beam (microstrain)

Location	Bottom plate (tension)		Top plate (compression)	
	Experiment	FE analysis	Experiment	FE analysis
600 mm from centre on left side	1,067	973	410	322
Centre	18,034	12,286	2,073	2,037
600 mm from centre on right side	1,272	971	401	324

Table 4 Comparison of strain values in lacings of LSCC-45 beam

Location	Tension		Location	Compression	
	Strain values, microstrain			Strain values, microstrain	
	Experiment	FE analysis		Experiment	FE analysis
IS1	31	61	IS2	120	189
IS3	65	136	IS4	83	175
IS6	13	51	IS5	101	149

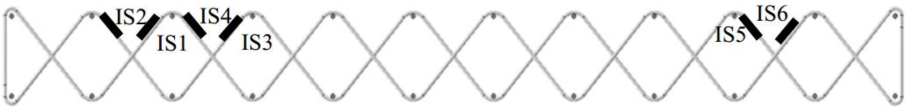

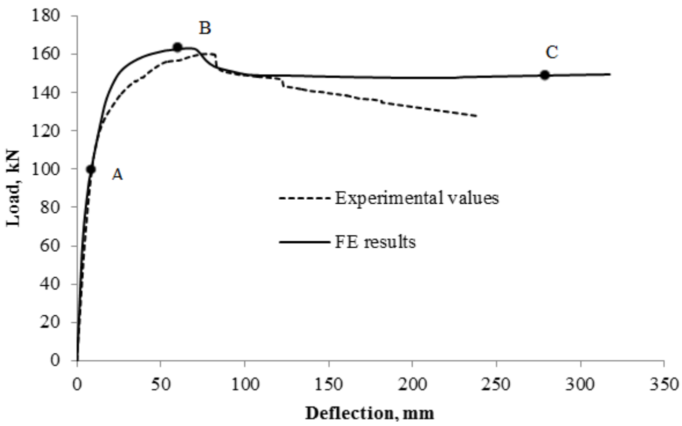

Fig. 10 Load-deflection behaviour of LSCC-60 beam

In addition to the load-displacement response, strain values are also considered for validation of the FE model. Strain values recorded in cover plates and lacings at different locations at maximum load are reported by Anandavalli *et al*. (2012). For the purpose of validation of FE model, strain values arrived numerically at the corresponding locations are compared with those measured experimentally for LSCC-45 beam as shown in Tables 3 and 4.

3.5.2 Load-Deflection Behaviour of LSCC-60 beam

Load-deflection values of LSCC-60 beam obtained using FE analysis is shown in Fig. 10.

From the load-displacement response, it is observed that in the initial elastic region upto 90 kN, FE analysis shows around 10% less deflection as compared to experimental values. With further increase in load, upto 125 kN, it is found that both numerical and experimental load-deflection values agree very well. With increasing load, FE model predicts about 20% less deflection than measured during the experiment upto ultimate load. Beyond ultimate load, post-peak response is found to deviate from experimental results. From FE analysis, ultimate load is observed as 163 kN, which is approximately 2% more than that obtained experimentally. In experiments, the post-peak response is found to have 18% drop in the load for maximum mid-span displacement of about 240 mm. From numerical analysis, drop in load for maximum mid-span displacement of about 315 mm is found to be around 8%.

Area of load-displacement curve obtained using FE analysis is approximately 40% more than that obtained from experiments. This is due to the fact that, failure stage has not been reached in experiments. For maximum mid-span displacement of about 315 mm, support rotation is calculated to be approximately 25° and ductility index is determined to be around 35.

Strain values predicted numerically in cover plates and lacings at specific locations are compared with the corresponding strains obtained from experiments for LSCC-60 beam as shown in Tables 5 and 6.

Table 5 Comparison of strain values in cover plates at maximum load of LSCC-60 beam (microstrain)

Location	Bottom plate (tension)		Top plate (compression)	
	Experiment	FE analysis	Experiment	FE analysis
600 mm from centre on left side	2,362	1,437	676	441
Centre	18,990	15,821	-	3,031
600 mm from centre on right side	1,819	1,438	566	442

Table 6 Comparison of strain values in lacings of LSCC-60 beam

Location	Tension		Location	Compression	
	Strain values, microstrain			Strain values, microstrain	
	Experiment	FE analysis		Experiment	FE analysis
IS6	345	445	IS5	68	228
IS1	411	500	IS2	115	500
IS3	91	287	IS4	300	569

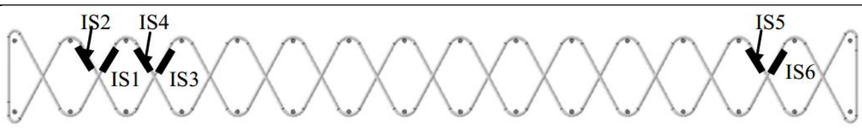

Table 7 Comparison of responses of LSCC beams

Parameter	LSCC-45 beam		LSCC-60 beam	
	Experimental	FE analysis	Experimental	FE analysis
Yield displacement	14.67 mm	8 mm	16 mm	9 mm
Displacement	169 mm at 13° rotation	146 mm at 13° rotation	240 mm at 16° rotation	230 mm at 16° rotation
Yield load	110 kN	90 kN	120 kN	100 kN
Peak load	150 kN	155 kN	160 kN	163 kN
Failure mode	Couldn't be ascertained	Tensile plate failure	Couldn't be ascertained	Tensile plate failure

3.5.3 Discussion on responses of two LSCC beams

From the response of two LSCC beams, it is noticed that concrete in the shear span region between loading points started cracking first and then yielding of bottom cover plate occurs. Even after yielding of bottom cover plate and cracking of concrete, the strains in lacings and cross rods are found to be less than the admissible limits. Strains in the top cover plate are found to be less than strains in bottom cover plate. Lacings help the cover plates to act together without making the system to fail.

Computed cover plate strains at maximum load are found to be less by than those recorded experimentally (about 30%). As per Tables 4 and 6, about 25% variation is seen in the strain values in the lacings. This can be attributed to the fact that in FE modelling, common nodes of steel plate, lacings and cross rods are merged at intersecting nodes, which is not the case in actual LSCC beam. In reality, lacings are being inserted through the perforations in the cover plate at appropriate places and made to stay intact by using cross rods. Table 7 gives the comparison of critical responses of LSCC beams obtained experimentally and numerically.

LSCC-60 beam is found to exhibit better performance in terms of displacement ductility and support rotation. Load carrying capacity of both beams is found to be more or less equal.

3.5.4 Critical stages of loading observed in LSCC-45 and LSCC-60 beams

In Figs 9 and 10, the points A,B,C show the critical stages of loading noticed in FE results. Point A denotes the point at which yielding of bottom cover plate initiated at a tensile strain of 0.0059 in case of LSCC-45 beam and 0.00541 in case of LSCC-60 beam. At this stage, stress in concrete in tensile zone crosses its cracking stress value, which denotes cracking of concrete. Peak loading stage is denoted by point B. At this stage, crushing of concrete occurs in the compression zone in shear span region for a strain of about 0.0035. In experiment also similar results were reported (Anandavalli et al. 2012).

Point C denotes the failure stage. Through FE analysis failure point is decided on the basis of tensile strain observed in bottom steel cover plate. LSCC beam is considered to fail when the tensile strain in bottom steel cover plate reaches its ultimate value of 0.2 (Anandavalli 2012). At this stage, strain values in lacings and cross rods are much lesser than its ultimate values. Though the strain in concrete crosses its crushing strain value, particular alignment of cover plates and lacings keeps the core intact without disintegration. Lacings remain active to transfer load between the cover plates, which this prevents the spalling of concrete.

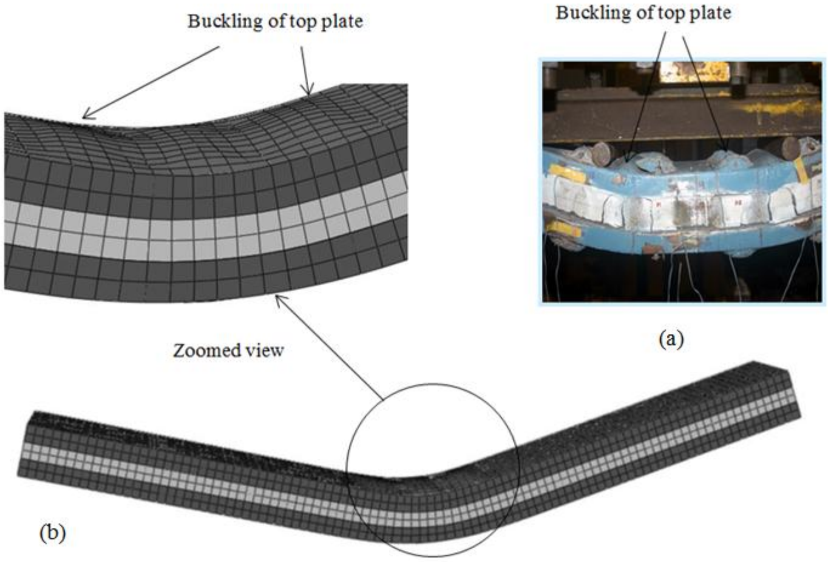

Fig. 11 Deflected shape showing buckling of top plates of LSCC-45 beam (a) Observed in experiment (Anandavalli *et al*. 2012); (b) Obtained through FE analysis

Table 8 Parameters considered in the study

Parameters	Abbreviation	Values
Plate thickness, mm	PT	2, 3, 4
Angle of lacing, degrees	LA	30, 45, 60
Concrete core grade, MPa	CG	25, 35, 60

Buckling of top plate is observed in the numerical analysis near the loading points at a load magnitude of about 100 kN in LSCC-45 beam and 135 kN in LSCC-60 beam. Similarly, in experiments buckling of top cover plate is reported near same location at a load level of 140 kN in LSCC-45 beam and 160 kN in LSCC-60 beam. Fig. 11 shows the buckling of top plate observed during experiment and numerical analysis.

4. Parametric analysis

Parametric study has been carried out to determine the most important parameter, which influences the response of LSCC beams. Parameters such as plate thickness, concrete grade and angle of lacing are considered in the study. LSCC beam of span 2.4 m, cross section 300 mm × 150 mm with simply supported boundary condition is used. Parameters considered and values used in the study are given in Table 8.

4.1 Effect of angle of lacing

Since the developed FE model has been validated with the experimental results, same model is adopted for parametric analysis. Now, FE analysis is carried out with lacing angle of 30°, plate

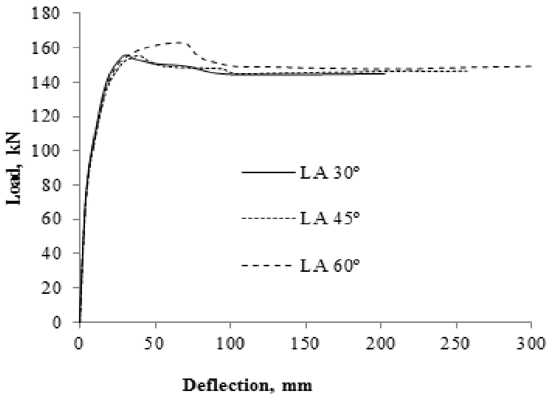

Fig. 12 Comparison of Load-deflection responses of LSCC beam with different lacing angles

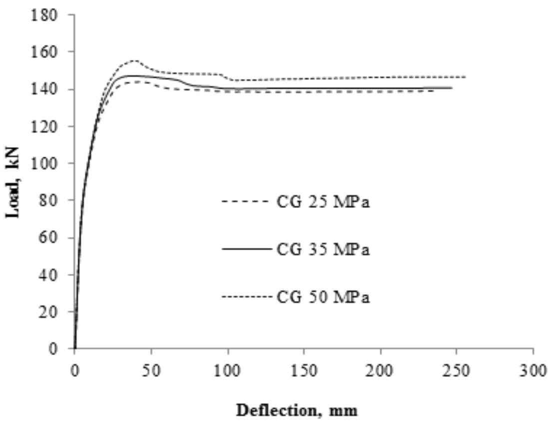

Fig. 13 Comparison of load-deflection responses of LSCC-45 beam with three concrete grades

thickness of 3 mm and concrete grade of 50 MPa. All other parameters are kept the same. LSCC beam is subjected to two-point loading, load is applied under displacement control mode. Comparison of Load-deflection responses of LSCC beam with three different lacing angles is shown in Fig. 12.

Load carrying capacity of all three beams is found to be more or less equal (i.e., around 160 kN). Maximum deflection achieved by the beams varies with the angle of lacing. Thus, LSCC-30 beam is found to exhibit least performance in terms of displacement ductility and support rotation. It can be concluded that angle of lacing places major role in ductility response of LSCC beams.

For design purpose, based upon the demand on ductility criteria and fabrication convenience, one can choose appropriate lacing angle.

4.2 Effect of concrete grade

LSCC-45 beam is chosen and FE analysis is carried out with varying grade of concrete (25, 35 and 50 MPa). Comparison of load-deflection responses of LSCC-45 beam with three different concrete grades is shown in Fig. 13.

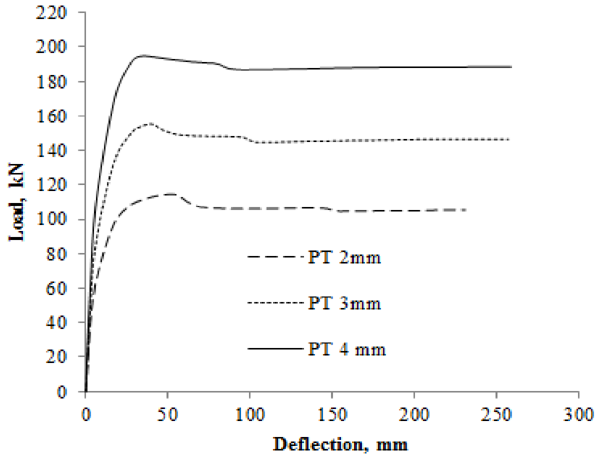

Fig. 14 Comparison of load-deflection responses of LSCC-45 beam with different cover plate thickness

It is observed that maximum displacement capacity is not significantly affected by change in grade of concrete unlike that of variation in angle of lacing. Only minimum variation in load carrying capacity is found with change in grade of concrete used. With increase in concrete grade, peak load carrying capacity is found to increase.

4.3 Effect of cover plate thickness

LSCC-45 beam is chosen and FE analysis is carried out with varying cover plate thickness of 2, 3 and 4 mm. Comparison of load-deflection responses of LSCC-45 beam with three cover plate thicknesses is shown in Fig. 14.

It is noticed that displacement capacity is not much influenced by the cover plate thickness. But tremendous change in peak load is observed with the variation in plate thickness. LSCC beam with larger plate thickness is found to possess better performance in terms of load carrying capacity.

5. Conclusions

Numerical model for determining the deformation capacity of LSCC beam under monotonic loading is developed by using FE analysis software ABAQUS. The FE model is found to provide better insight into realistic behaviour of LSCC beams (including yielding of cover plates, crushing of concrete and buckling of top cover plate). Validation of the FE model is carried out by comparison with the experiments results generated by the authors and the model is found to be effective in terms of predicting load-deflection behaviour, post-peak behaviour and different failure stages of LSCC beams subjected to monotonic loading. The failure mode is established as the tensile strain in bottom cover plate reaching the corresponding ultimate value. The deformation capacity of the beam represented by support rotation and ductility denote very high value, when compared to the conventional reinforced concrete beam. The specific large deformation capacity of LSCC beam is attributed to the particular geometry and the integration of elements in LSCC beam. Parametric studies conducted leads to the conclusion that plate thickness significantly influences the load carrying capacity and maximum deflection achieved is influenced by the angle of lacing. Thus from design point of view, based upon the requirement one can adopt appropriate lacing angle and plate thickness, keeping fabrication feasibility also in mind.

Acknowledgments

The authors wish to acknowledge the technical discussions with their colleagues of Shock and Vibration Laboratory, CSIR-Structural Engineering Research Centre (SERC), Chennai. This paper is being published with the kind permission of the Director, CSIR-SERC, Chennai, India.

References

Anandavalli, N. (2012), "Experimental and analytical studies on laced reinforced concrete and laced steel concrete composite elements", Ph.D. Thesis; Department of Civil Engineering, Anna University, Chennai, India.

Anandavalli, N., Lakshmanan, N., Iyer, N.R., Samuel Knight, G.M. and Rajasankar, J. (2011), "A novel modelling technique for blast analysis of steel-concrete composite panels", *Procedia Engineering*, **14**, 2429-2437.

Anandavalli, N., Lakshmanan, N., Samuel Knight, G.M., Iyer, N.R. and Rajasankar, J. (2012), "Performance of laced steel-concrete composite (LSCC) beams under monotonic loading", *Eng. Struct.*, **41**, 177-185.

Attard, M.M. and Setunge, S. (1996), "The stress-strain relationship of confined and unconfined concrete", *ACI Materials Journal*, **93**(5), 432-442.

Au, F.T.K. and Bai, Z.Z. (2007), "Two-dimensional nonlinear finite element analysis of monotonically and non-reversed cyclically loaded RC beams", *Eng. Struct.*, **29**(11), 2921-2934.

Bowerman, H., Coyle, N. and Chapman, J.C. (2002), "An innovative steel-concrete construction system", *The Structural Engineer*, **80**(20), 33-38.

Clubley, S.K., Moy, S.S.J. and Xiao, R.Y. (2003a), "Shear strength steel-concrete-steel composite panels. Part I-testing and numerical modelling", *J. Construct. Steel Res.*, **59**(6), 781-794.

Clubley, S.K., Moy, S.S.J. and Xiao, R.Y. (2003b), "Shear strength steel-concrete-steel composite panels. Part II-Detailed numerical modelling of performance", *J. Construct. Steel Res.*, **59**(6), 795-808.

Foundoukos, N. and Chapman, J.C. (2008), "Finite element analysis of steel-concrete-steel sandwich beams", *J. Construct. Steel Res.*, **64**(9), 947-961.

Guo, Z. and Zhang, X. (1987), "Investigation of complete stress-deformation curves for concrete in tension", *ACI Journal*, **82**(3), 310-324.

Jankowiak, T. and Lodygowski, T. (2005), "Identification of parameters of concrete damage plasticity constitutive model", *Found. Civil Environ. Eng.*, **6**(1), 53-69.

Leekitwattana, M. (2011), "Analysis of an alternative topology for steel-concrete-steel sandwich beams incorporating inclined shear connectors", Ph.D. Thesis; Faculty of Engineering, Science and Mathematics, University of Southampton, UK.

Liew, J.Y.R. and Sohel, K.M.A. (2009), "Lightweight steel – concrete –steel sandwich system with J-hook connectors", *Eng. Struct.*, **31**(5), 1166-1178.

Liew, J.Y.R., Sohel, K.M.A. and Koh, C.G. (2009), "Impact tests on steel-concrete-steel sandwich beams with lightweight concrete core", *Eng. Struct.*, **3**(9), 2045-2059.

Luo, Y., Li, A. and Kand, Z. (2012), "Parametric study of bonded steel-concrete composite beams by using finite element analysis", *Eng. Struct.*, **34**, 40-51.

Machacek, J. and Studnicka, J. (2002), "Perforated shear connectors", *Steel Compos. Struct., Int. J.*, **2**(1), 51-66.

Sohel, K.M.A., Liew, J.Y.R., Alwis, W.A.M. and Paramasivam, P. (2003), "Experimental investigation of low-velocity impact characteristics of steel-concrete-steel sandwich beams", *Steel Compos. Struct., Int. J.*,

3(4), 289-306.
Tomlinson, M., Tomlinson, A., Chapman, M.L., Jefferson, A.D. and Wright, H.D. (1989), “Shell composite construction for shallow draft immersed tube tunnels”, *Proceedings of the ICE International Conference on Immersed Tube Tunnel Techniques*, Manchester, UK, April.

CC